OPEN ACCESS INTERNATIONAL JOURNAL OF SCIENCE & ENGINEERING

# FUZZY BASED MAXIMUM POWER POINT TRACKING METHOD FOR PV ARRAYS UNDER PARTIAL SHADING CONDITIONS

**[1]Chippala Ravi [2]Dr. Ch. Ravi Kumar**

*[1]M.Tech Scholar of Power System Engineering, Department of EEE, Acharya Nagarjuna University.*

*[2]Assistant Professor, Department of EEE, Acharya Nagarjuna University.*

*chravicare4u@gmail.com ravikumarchekka@gmail.com*

***Abstract: This paper presents the fuzzy logic based maximum power point tracking for the optimization of the solar photovoltaic (PV)array under partially shaded conditions. The PV system is modelled in MATLAB/SIMULINK where the PV array is formed by three PV modules connected in series. The P V characteristic of PV module and PV array under uniform solar irradiance are nonlinear but there are one maximum power point (MPP) can be identified. Nevertheless, the P V characteristic becomes more complex with multiple MPP when the PV array under partially shaded conditions (PSC). In this paper, maximum power point tracking (MPPT) approach based on Hill climbing algorithm has been investigated. Fuzzy logic is adopted into the conventional MPPT to enhance the overall performance of the PV system. The performances of MPPT and FMPPT are investigated particularly on the transient response and the steady state response when the PV array is exposed under different partially shaded conditions. The simulation results show that FMPPT has better performance where it can facilitate the PV array to reach the MPP faster and provide more stable output power.***

***Keywords***-*photovoltaic; Partially shaded conditions; fuzzy logic; MPPT*

∴∴∴

## I INTRODUCTION

NOWADAYS, solar energy as a clean and free available renewable energy resource is too important for reducing the dependency on conventional sources. Photovoltaic (PV) systems produce electric power by directly transforming the in- exhaustible solar energy into electricity. However, the relatively high cost, low conversion efficiency of electric power generation, dependency on environmental conditions (e.g., solar irra+diance and temperature), and nonlinearity of the power–voltage (P–V) and current-voltage (I–V) characteristic of PV arrays are the main challenges in utilization of PV arrays.

Tracking the global peak (GP) of a PV array in all conditions is significantly important to guarantee the maximum achievable power. Many maximum power point tracking (MPPT) methods have been proposed in the literature [1]–[3]. Popular MPPT methods like perturbation and observation (P&O), hill climbing (HC), and incremental conductance (IC) methods are shown to be effective when the solar irradiance condition is uniform for all PV modules. Since, the tracking becomes more complicated un- der partial shading conditions (PSCs), i.e., when all the modules do not receive uniform solar irradiance, these basic methods fail to track the GP. Though in uniform solar irradiance conditions the P-V characteristic of PV array has just one peak, the P- V characteristic of PV array displays multiple peaks under PSCs. Hence, several MPPT methods are proposed which are applicable in PSCs. These methods can be categorized into two groups: hardware-based methods and software-based methods[4].

In [5] and [6], a controller is assigned for each module. These hardware-based methods can resolve the problem, since the P-V characteristic of a module (with just one bypass diode) always has a single peak. These methods, however, are not cost-effective and require much more devices in comparison to software-based algorithms.

In [4], the HC method has been improved. It can efficiently detect the shading condition. Then, by measuring power in suit- able points, it chooses the highest one and performs the HC around this point.

However, it does not have an acceptable accuracy for tracking the GP, since it compares the power of points near the LPs instead of the LPs themselves. In [7], a modified P&O method has been introduced which benefits from a unique characteristic that has been observed in the P-V curves. Although it has a great performance, since almost two measurements are done for each LP, the tracking speed is low. In [8], it is claimed that the GP is around the intersection of the I- V characteristic of PV arrays and a certain line. It depends on short circuit current of array which is problematic [1]. This problem is almost resolved by updating this value based on the solar irradiance. However, it is uncommon to find sensors that measure solar irradiance levels [1]. In [9], a relationship is defined between the PV power and a control signal to track the P-V curve and find the GP. Although its accuracy is high, it is slow because it searches almost all the range of the P-V curve. The proposed method in [10] uses the critical observations reported in [7] in a different way, but it does not have any procedure for detecting whether there is an LP near the target point or not. As a result, it may fail in some PSCs. two methods are proposed. The first one searches the P-V curve for MPPs by means of IC. However, it skips parts of the area based on short circuit current of the modules and the highest local power. This method would be very slow since it must scan almost all the P-V curve. Although the second method has improved the speed of tracking compared to the first one, it still uses one current sensor for each bypass diode, which is not cost effective Proposing a method which meets accuracy, convergence speed, simplicity, minimum needed parameters, minimum cost and other important factors

[1] at the same time is still of a great importance. In this paper, we propose a novel method for MPPT of PV arrays which works effectively in PSCs and at the same time, has great performance in diverse factors mentioned above. By measuring PV current in defined points, the method maps out the solar irradiance pattern. Based on the mapping, it chooses appropriate points for tracking the LPs. Then, it performs HC in these points and tracks all the LPs. Finally, by comparison of the acquired LPs, it chooses the GP

## II I-V CHARACTERISTIC OF PV ARRAYS UNDER PSCS

### *A. Single-Diode Model:*

Based on the single diode model of the PV cells, if $N_s$ modules (each of which consists of $N_{s,m}$ series cells) are serried, and $N_p$ strings are paralleled, the voltage equation of the array would be as follows[15].

$$V = N_s\left(\frac{akTN_{s,m}}{q}\right)\ln\left[\frac{I_{\mathrm{pv,array}} - I}{I_{0,\mathrm{array}}}\right] - \left(\frac{N_s}{N_p}\right)R_sI \quad (1)$$

W

$V$ and $I$ are the output voltage and current of PV array, respectively. $I_{pv,array}$ is the output current of PV array. $I_{0,array}$ is the equivalent saturation current. $q$ is the electron charge (1.60217646 $10^{-19}$ $C$), $k$ is the Boltzmann constant (1.3806503*$10^{-23}$ $J/K$), $T$ is the junction temperature in Kelvin, and $a$ is the diode ideality constant. $R_S$ is the PV module's series resistance.

For $I_{pv,array}$ and $I_{0,array}$ we can have [4]

$$I_{\mathrm{pv,array}} = N_p \overbrace{\left(I_{\mathrm{scn},m} + K_I\Delta T\right)\frac{G}{G_n}}^{I_{\mathrm{sc},m}} \quad (2)$$

and

$$I_{0,\mathrm{array}} = N_p\frac{\left(I_{\mathrm{scn},m} + K_I\Delta T\right)}{\exp\left[\frac{q(V_{\mathrm{ocn,m}} + K_V\Delta T)}{akTN_{s,\mathrm{m}}}\right] - 1} \quad (3)$$

where $I_{scn,m}$ is the short-circuit current of the module in standard test condition (STC), $I_{sc,m}$ is the short circuit of module in real condition, $K_I$ is the current coefficient, $G$ is the solar irradiance level (W/m$^2$), and $ttn$ is the nominal solar irradiance level (1000 W/m$^2$). $\Delta T$ is the temperature difference to temperature of STC. $V_{ocn,m}$ is the module open circuit voltage in STC and $K_V$ is the voltage coefficient. Since

$$\exp\left[\frac{q(V_{\mathrm{ocn},m} + K_I\Delta T)}{akTN_{s,m}}\right] >>> 1 \quad (4)$$

(3) can be simplified as

$$I_{0,\mathrm{array}} = N_p\frac{\left(I_{\mathrm{scn},m} + K_I\Delta T\right)}{\exp\left[\frac{q(V_{\mathrm{ocn,m}} + K_I\Delta T)}{akTN_{s,\mathrm{m}}}\right]}. \quad (5)$$

Substituting (2) and (5) into (1) yields

$$V = N_s\left(\frac{akTN_{s,m}}{q}\right)\ln\left[\frac{G}{G_n} - \frac{I}{N_p(I_{\mathrm{scn},m} + K_I\Delta T)}\right] + N_s\overbrace{\left(V_{\mathrm{ocn},m} + K_V\Delta T\right)}^{V_{\mathrm{oc,m}}} - \left(\frac{N_s}{N_p}\right)R_sI \quad (6)$$

where $V_{\mathrm{oc},m}$ is module's open-circuit voltage in real condition. Having $I_{\mathrm{pv,array}} \approx I_{\mathrm{sc,array}}$ [21], [23], (2) can be rewritten as

$$I_{\mathrm{sc,array}} = N_p \overbrace{\left(I_{\mathrm{scn},m} + K_I\Delta T\right) \times \frac{G}{G_n}}^{I_{\mathrm{sc,m}}} \quad (7)$$

Where Isc,array is the short circuit current of array

### *B.I-V Characteristic of PV Arrays Under PSCs:*

Fig. 1 shows the I-V characteristic of a sample 3*2 array under different PSCs. The modules' parameters are listed in Table I. The modules are modeled based on single diode model in [16] and the equivalent parameters of PV modules are listed in Table II. $Rp$ is the PV module's parallel resistance. As illustrated in Fig. 1, the value of the current in each step is almost constant up to the end of that step. Keeping this point in mind, by measuring the PV current in specific points and comparing them in a suitable manner which are presented in section III, the PSC pattern can be mapped. As a result, the number of steps, their lengths, and their order in the I- V characteristic can be detected. In addition, as it is depicted in Fig. 1, voltage values in the starting points of current steps, are in near left-side neighborhood of certain integer multiples of $V_{oc,m}$ . In order to justify above claim, a sample PV array consists of two strings each of which includes three series modules, is considered as shown in Fig. 2. The modules' parameters are given in Tables I and II. Since the test is executed under STC, $\Delta T$ equals tozero and $V_{oc,m}$ equals to $V_{ocn,m}$ which is 11.15 V.Also, Fig. 3 demonstrates the I-V characteristic of each group as well as the total characteristic of the PV array.

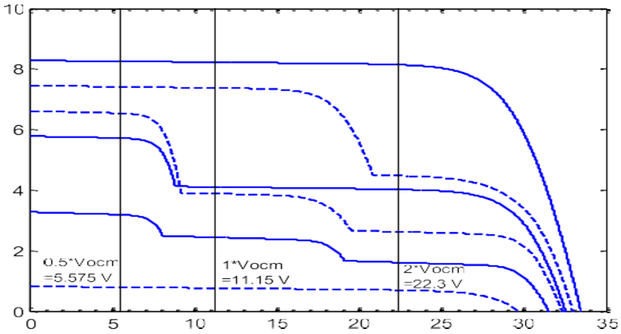

Fig. 1. I-V characteristic of a sample 3*2 array under different PSCs when the module open circuit voltage and short circuit current are based on Table 1

TABLE I PV MODULE'S PARAMETERS

| Parameter | VALUE |
|---|---|
| $P_{MPP}$ | 35 W |
| $V_{oc,n}$ | 11.15 V |
| $I_{sc,n}$ | 4.15 A |
| $N_{s,m}$ | 18 |

TABLE II EQUIVALENT PARAMETERS OF PV MODULE IN SINGLE DIODE MODEL [16] IN STC

| Parameter | VALUE |
|---|---|
| a | 1.077 |
| Rs | 0.175 Ω |
| Rp | 123 Ω |

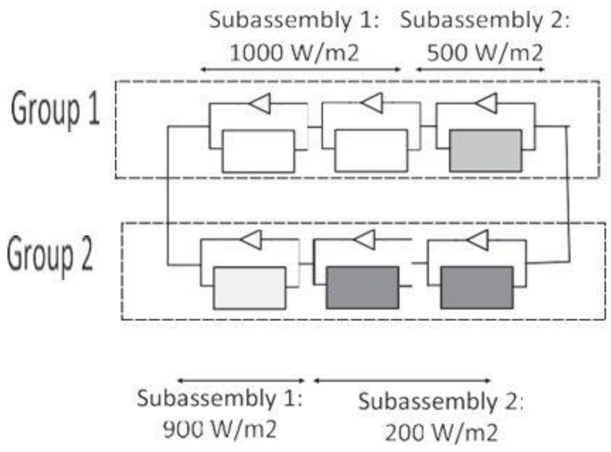

Fig. 2. Sample 3 × 2 PV array under PSC.

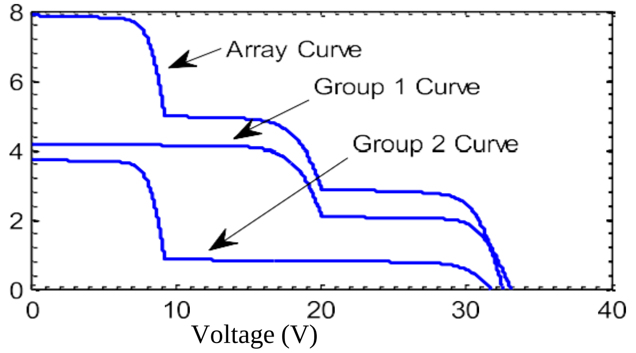

Fig. 3. I-V characteristic of group 1, Group 2, and total array in Fig. 2.

***1) Group 1 Analysis:*** The value of the voltage in the starting point of the second step of group 1 can be derived from the voltage of subassembly 1 and 2 in this point:

$$V_{beginning,St2G1} = V_{Sub1G1} + V_{Sub2G1} \quad (8)$$

where $V_{beginning,S\ t2tt1}$ stands for the voltage of the starting point of the second step in group 1. $V_{Sub1tt1}$ and $V_{Sub2tt1}$ are the voltages of subassembly 1 and 2 in this point, respectively. It should be noticed that in this point, the bypass diode of the module in subassembly 2 is still ON and is going to be OFF. Therefore, the voltage of subassembly 2 in this point derives from the bypass diode's forward voltage, which is 0.8 V in this test

$$V_{Sub2G1} = -0.8 \text{ V}. \quad (9)$$

Using (7), the short circuit current of the subassembly 2 can be determined as the following equation. In this case $G = 500$, $\Delta T = 0$, and $N_p = 1$

$$I_{sc,Sub2G1} = 2.075 \text{ A} \quad (10)$$

where $I_{sc,Sub2G1}$ stands for open-circuit voltage of the sub- assembly 1 of group 1. Using (6), the corresponding voltage of the subassembly 1 in the start point of the second step can be calculated. In this case

$G =$ 1000, $\Delta T$ = 0, $T$=298.15 K, $N_s$ =

2, $N_p$ = 1, and $V_{ocn,m}$ = 11.15 V. Also, the value of $I$ in (6) equals to 2.075 A, since the starting point of the second step is the end of the first step. Therefore, one can write

$$V_{Sub1G1} = 20.883\ \text{V}. \qquad (11)$$

Substituting (9) and (11) into (8) yields

$$V_{beginning,St2G1} = 20.083\ \text{V}. \qquad (12)$$

As it was claimed, the starting point of the second step (20.083 V) is in near left side neighborhood of certain integer multiple of $V_{oc,m}$ which is 2 $V_{oc,m}$ (22.3 V) in this case.

***2) Group 2 Analysis:*** The analysis of this group is similar to analysis of group 1. So, the value of the voltage in starting point of the second step of group 2 can be derived from the voltage of subassembly 1 and 2 in this point

$$V_{beginning,\ St2G2} = V_{Sub1G2} + V_{Sub2G2} \ (13)$$

where $V_{beginning,\ St2G2}$ stands for the voltage of the starting point of the second step in group 2. $V_{S1G2}$ and $V_{S2G2}$ are the voltages of subassembly 1 and 2 in this point, respectively. In this point the bypass diodes of the modules in subassembly 2 are still ON and are going to be OFF. Then, the voltage of subassembly 2 in this point derives from the bypass diode’s forward voltage, which is 0.8 V in this test

$$V_{Sub2G2} = -1.6 \qquad (14)$$

The short circuit of the subassembly 2 can be calculated using (7). In this case $G = 200$, $\Delta T = 0$, and $Np = 1$

$$I_{sc,\ Sub2G2} = 0.83\ A \ (15)$$

where Isc, Sub2G2 stands for open-circuit voltage of the subassembly 1 of group 2. Again by usage of (6), the corresponding voltage of the subassembly 1 in the starting point of the second step can be calculated. In this case G = 900, ΔT = 0, T = 298.15 K, Ns = 1, Np =1, and Vocn,m = 11.15 V.

Also, the value of I in (6) equals to 0.83 A. Therefore,

$$V_{Sub1tt2} = 10.827\ \text{V}. \qquad (16)$$

Substituting (14) and (16) into (13) yields

$$V_{beginning,S_{t2G\ 2}} = 9.227\ \text{V}. \qquad (17)$$

Similar to group 1, the starting point of the second step (9.227 V) in group 2 is in near left side neighborhood of certain integer multiple of Voc,m which is 1 Voc,m (11.15 V) in this case.

3)Array Analysis: Since the curves of each group consist of steps in which the values of current are almost constant until the next step, the summation value would also have this characteristic. On the other hand, since the starting points of the total curve are the starting points of the steps in groups 1 and 2, the value of the voltage for each start point is in near left side neighborhood of a certain multiple of Voc,m . The proposed analysis is valid for every structure.

## III PROPOSED METHOD FOR MPPT

Fig. 4 shows the flowchart of the proposed method. In steady state conditions, the HC method performs around the last GP which has been detected by the proposed method.

### A.Detecting the Solar Irradiance Changes:

In order to recognize the sudden changes of the solar irradiance condition, the power difference between each two consecutive cycles (ΔP) is calculated and compared against a certain critical power variation (ΔPcrit), as illustrated in Fig. 4. If ΔP is higher than ΔPcrit, variation of the solar irradiance condition is detected and the global MPPT starts. Generally, the sudden changes in solar irradiance are small in magnitude (smaller Than 27 W/m2) [7]. So, ΔPcrit can be equal to the change in output power of array, for the condition that the solar irradiance changes by 27 W/m2 [7]. Or, it might be set to an appropriate- ate percentage of array nominal power [7]. In this paper, this threshold is set to 5% of the nominal power, based on trial and error observation from simulation. Once the solar irradiance change is detected, the sections B and C in Fig. 4 start to track the new GP as explained in the following.

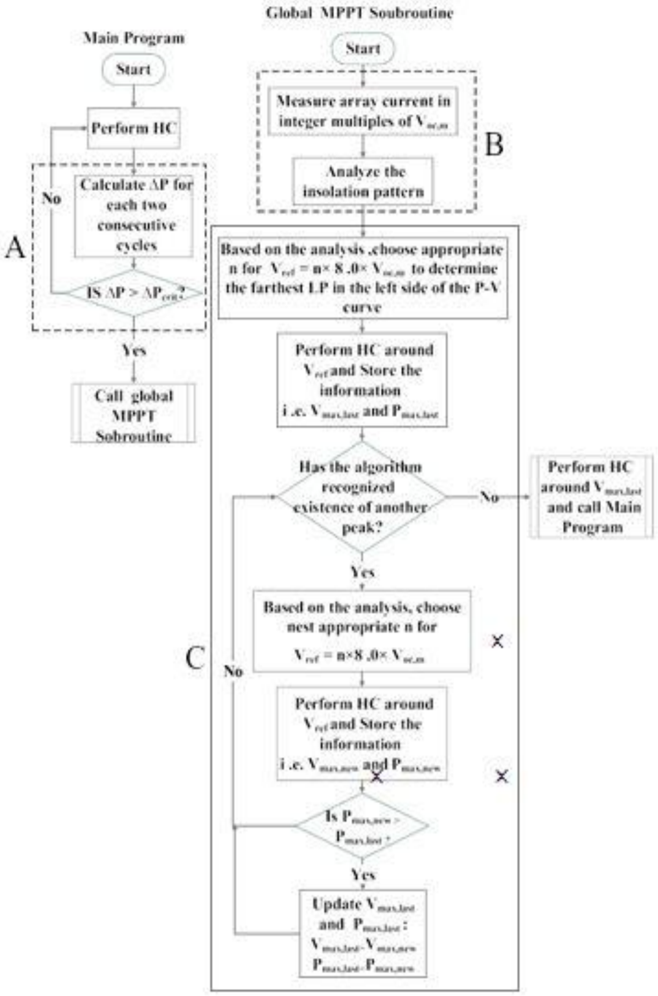

Fig. 4. Flowchart of the proposed method.

*A. Analysis of the Solar Irradiance pattern:*

In Section B, the method measures the current in the multiples of $V_{oc,m}$ . It was proved in Section II-B that the starting point of the current steps in the I-V characteristic are in the near left side neighbourhood of certain integer multiples of $V_{oc,m}$ . In addition, the value of the current for each step is nearly constant up to the next step. Therefore, by comparing the measured currents against each other, the number of steps, their lengths, and their order in the I-V characteristic can be easily determined by the following procedure.

If $I_{Vk}$ is the measured current in $K\ V_{oc,m}$ and $I_{V(k-1)}$ is the measured current in $(K\ 1)\ V_{oc,m}$ , the proposed method checks the validity of the following inequality:

$$\frac{I_{V(k-1)} - I_{Vk}}{I_{V(k-1)}} \le \Delta I_{crit}. \qquad (18)$$

If this inequality is satisfied, the proposed method recognizes that there is no new step in the neighborhood of $K\ {*}V_{oc,m}$ ; otherwise the new step is detected by the method. It should be noticed that if the steps were ideal, i.e., the I-V characteristic was constructed from rectangular sections, $\Delta I_{crit}$ must be zero. However, the steps are not ideal. Since the current source part of the I-V characteristic of the PV array under uniform conditions continues to maximum power point (in which current is about $0.9{*}I_{sc}$ [7], [14]), an appropriate value for $\Delta I_{crit}$ is $(I_{sc}-0.9{*}I_{sc})/I_{sc}$ which equals to 0.1. Generally, lower values of $\Delta I_{crit}$ lead to higher accuracy, but it increases the time required to track the GP. Since the boost converter is used, it is better to keep distance from zero-voltage point and measure the current of $0.5{*}V_{oc,m}$ instead of the current of zero voltage point. However, measuring the current in a small voltage makes the boost converter to work in a relatively large duty cycle and it is a drawback.

It is helpful to describe this procedure in a sample case. The corresponding I-V and P-V curves of a 3*2 PV array whose parameters are listed in Tables I and II, under a sample PSC are shown in Fig. 5(a) and (b), respectively. For analyzing the PSC pattern, the current of PV array is measured in three points ($2{*}V_{oc,m}$ , $1{*}\ V_{oc,m}$ , and $0.5{*}V_{oc,m}$ ). As it is depicted in Fig. 5(a), these three points are $P_1$ (22.3 V, 6.13 A), $P_2$ (11.15 V, 8.2 A), and $P_3$ (5.575 V, 8.24 A), respectively.

(18) is checked for corresponding currents as follows:

$$\frac{8.24 - 8.2}{} = 0\ 005 \le 0\ 1 \quad (19)$$

8.24

$$\frac{8.2 - 6.13}{8.2} = 0.25 > 0.1 \qquad (20)$$

Hence, based on the described procedure, the algorithm recognizes that there are two steps in the I-V curve, with the lengths of $L_1$ ($2{*}V_{oc,m}$ ) and $L_2$ ($1{*}V_{oc,m}$ ). Actually, (18) is true in the case that $k = 1$ which means that $P_3$ and $P_2$ are in the same step. Since (18) is not satisfied in the case that $K = 2$, it means that $P_1$ and $P_2$ are not in the same steps. Thus, as it was claimed, the proposed method detects the number of steps, their lengths, and their order in the I- V characteristic with just measuring the array current. This new idea is very simple and yet so useful for MPPT in PSCs. It should be mentioned that, although methods like [12] use one voltage sensor for each module to map out the PSC pattern, the new method maps out the PSC pattern with just one current sensor.

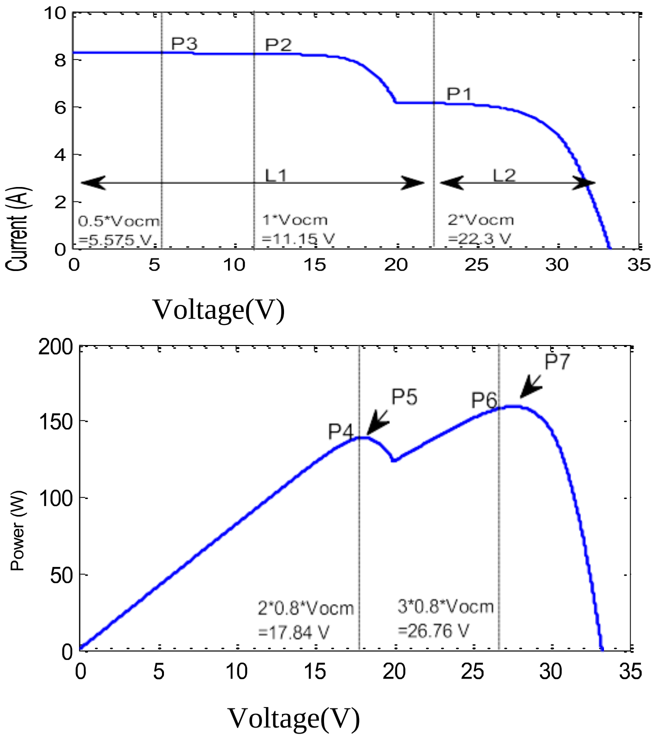

Fig. 5. (a) I-V characteristic and (b) P-V characteristic of a sample 5 × 5 array.

*B. Searching for Maximum Power Points:*

Based on [7], the LPs are in neighborhood of integer multiples of $0.8 * V_{oc,m}$ . So according to the analyzed solar irradiance pattern, the method allocates a certain multiple of $0.8 * V_{oc,m}$ , to each LP. Thus by operation of the HC method in its neighborhood, the corresponding LP is tracked. Finally, by comparison among the LPs, the GP is determined.

Whether each LP is tracked or not is recognized by checking the slope of the P-V curve. After determining the largest LP as the GP, the HC is performed around it. When the GP is tracked, the duty cycle is fixed to prevent the perturbations, as discussed in [9]. However, it is not necessarily an issue for the proposed method. Besides, a variable step HC can be used to decrease the perturbations around the GP.

To better understand the above procedure, the previous example is considered for finding the GP. After obtaining the PSC pattern, the HC is performed around $P_4$ (17.84 V) in which voltage equals to $L_1 * 0.8 * V_{oc,m}$ ($2 * 0.8 * V_{oc,m}$), and tracks $P_5$ (138.9 W), as it is illustrated in Fig. 5(b). Then, based on the obtained PSC pattern, the algorithm goes to the neighborhoods of the other LP, i.e., $P_6$ (26.76 V) in which voltage equals to $(L_1 + L_2) 0.8 * V_{oc,m}$ ($3 * 0.8 * V_{oc,m}$). The HC method is performed around this point and the other LPs are tracked, which are P7 (170 W). Finally, by comparison among these LPs, the GP which is P6 (159.3 W) is determined.

Since the proposed method is a search-based tracking algorithm and just initiates the HC method in×the neighborhood of 0.8 * Voc,m , it does not really depend on the open circuit voltage. But the voltage can be updated every 10 min by the following equation [4]:

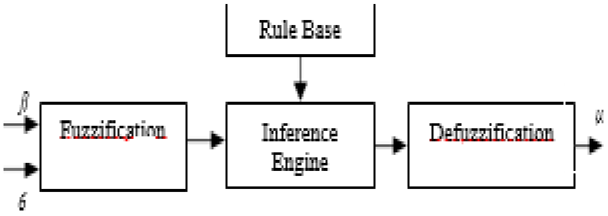

Fig. 4. Operation of fuzzy logic control.

$$V_{oc,m} = V_{ocn,m} + K_V \Delta T \quad (21)$$

and after each update, the proposed method can be performed.

As described, the proposed algorithm has modified the conventional HC method to work properly in PSCs. Therefore, it is simple for experimental implementation. Also, as presented in subsequent sections, the accuracy and convergence speed of the proposed method are better than existing methods.

| Table.3 System's Parameters | |
|---|---|
| Parameter | Valve |
| L | 0.6mH |
| Cin | 34uF |
| Cout | 48uF |
| Switching frequency | 40KHz |
| Sampling frequency | 1KHz |
| Array nominal open circuit voltage | 33.45v |
| Array nominal short circuit voltage | 8.3A |
| Array nominal power | 210W |

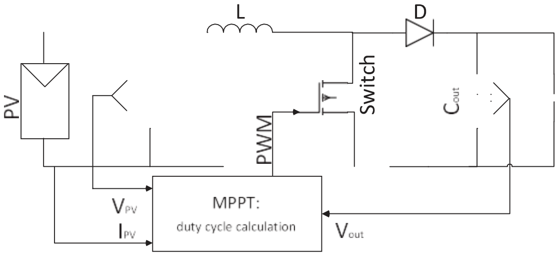

Fig. 6. Schematic of the system

## IV FUZZY LOGIC:

Fuzzy logic is well known as a logical system that does not require accurate mathematic model. Fuzzy logic implements linguistic variable computing method rather than the precise numerical digit numbers. In other words, fuzzy is able to function properly even without precise inputs. Fuzzy logic is relatively more robust compared to the conventional nonlinear controller.

There are four basic elements in the operation of fuzzy logic control, known as the fuzzification, the rule base, the inference engine and the defuzzification. The operation of fuzzy logic control is shown in Fig. where the fuzzy logic control has two inputs, ß and 6 and one output, µ

The operation of fuzzy logic control is initiated by the fuzzification. Fuzzification is the progression of converting the inputs into linguistic variable. Referring to Fig., the PV system actual signal *ß* and *6* will be converted into linguistic fuzzy sets via fuzzification. The linguistic fuzzy sets will be represented by fuzzy membership function which it is a curvature presenting each and every point of the membership value. The fuzzy rule base is a compilation of every if-then rules. The rule base contains all information for the controlled parameters and judges all the possible outcomes. The rules are defined according to the professional knowledge and experience on the operation of the system control. The fuzzy inference engine has the capability on decision making where the judgment is based on the defined fuzzy rules. The inference engine is therefore transforming×the fuzzy rule base into fuzzy linguistic output. Subsequently, the defuzzifier transferred the linguistic fuzzy sets back into the actual value of $\mu$.

Fuzzy logic is adopted in the HC algorithm to increase the flexibility of the algorithm in varying the size of the hill voltage, $\Delta V$. When the fixed hill size $\Delta V$ is small, the PV array will suffer from slow tracking of MPP. Increasing perturbation size of $\Delta V$ will cause large oscillation on the PV array's operating voltage and subsequently causing power fluctuation problem in the system. With the assistance of fuzzy logic, FMPPT is able to adjust the perturbation size of $\Delta V$ based on the collected data at instantaneous circumstances. FMPPT can control the PV array to have fast transient response hence the maximum power operating condition can be tracked faster. In addition, FMPPT is able to reduce the oscillation of the operating voltage thus maintaining the power stability of the PV array when the MPP has been successfully identified.The configuration of membership function is not set to be distributed evenly along the universe of discourse. As shown in Fig., the output variable has three membership functions in the range of [0 1] whereas only one membership functions are defined in the range of [0.8 2]. This is because fuzzy logic has been placed to work more sensitive in the range of [0 1], where fuzzy logic will decide a smaller but precise size of perturbed voltage when the PV array is approaching MPP.

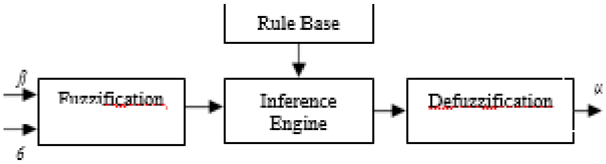

Fig. 4. Operation of fuzzy logic control.

The membership functions of the input variables are matched with the membership functions of the output variable forming fuzzy rule base system. The rules are validated through fuzzy viewer by adjusting the index line. This process is to verify the fuzzy computed *AV* to be same as the desired value.

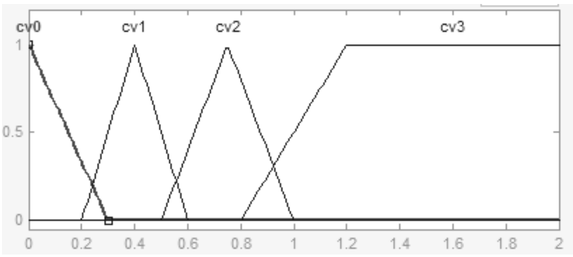

Fig. Membership function of the fuzzy output variable *AV*

## V SIMULATION RESULTS

In this section several simulation results will be presented. The simulated PV system is a 3 2 PV array, whose parameters are listed in Tables I and II.

The PV array is connected to a boost DC-DC converter which tracks the maximum power point. There are three series connected 12-V batteries in the output side. The parameters of system under study are listed in Table III. Also the schematic of the system is shown in Fig. 6.

During adoption of HC method, the duty cycle of the boost converter is calculated directly based on the last duty cycle as follows:

$$Dk = Dk - 1 + dk \quad (22)$$

where *D* and *D* are the calculated duty cycles in previous (k-1 th) and present (kth) cycle, respectively.dk is a number which it's value is constant, but it's sign may change in each cycle. If the value of the power measured in the *K*th cycle is larger than the value of power measured in (*K*-1)th cycle, *dk* is calculated as

$$Dk = Dk - 1 \quad (23)$$

On the other hand, if the power in the *K*th cycle is smaller than the power in (*K*-1)th cycle, *dk* is

There are four basic elements in the operation of fuzzy logic control, known as the fuzzification, the rule base, the inference engine and the defuzzification. The operation of fuzzy logic control is shown in Fig. where the fuzzy logic control has two inputs, *ß* and *6* and one output, $\mu$

The operation of fuzzy logic control is initiated by the fuzzification. Fuzzification is the progression of converting the inputs into linguistic variable. Referring to Fig., the PV system actual signal *ß* and *6* will be converted into linguistic fuzzy sets via fuzzification. The linguistic fuzzy sets will be represented by fuzzy membership function which it is a curvature presenting each and every point of the membership value. The fuzzy rule base is a compilation of every if-then rules. The rule base contains all information for the controlled parameters and judges all the possible outcomes. The rules are defined according to the professional knowledge and experience on the operation of the system control. The fuzzy inference engine has the capability on decision making where the judgment is based on the defined fuzzy rules. The inference engine is therefore transforming×the fuzzy rule base into fuzzy linguistic output. Subsequently, the defuzzifier transferred the linguistic fuzzy sets back into the actual value of $\mu$.

Fuzzy logic is adopted in the HC algorithm to increase the flexibility of the algorithm in varying the size of the hill voltage, $\Delta V$. When the fixed hill size $\Delta V$ is small, the PV array will suffer from slow tracking of MPP. Increasing perturbation size of $\Delta V$ will cause large oscillation on the PV array's operating voltage and subsequently causing power fluctuation problem in the system. With the assistance of fuzzy logic, FMPPT is able to adjust the perturbation size of $\Delta V$ based on the collected data at instantaneous circumstances. FMPPT can control the PV array to have fast transient response hence the maximum power operating condition can be tracked faster. In addition, FMPPT is able to reduce the oscillation of the operating voltage thus maintaining the power stability of the PV array when the MPP has been successfully identified. The configuration of membership function is not set to be distributed evenly along the universe of discourse. As shown in Fig., the output variable has three membership functions in the range of [0 1] whereas only one membership functions are defined in the range of [0.8 2]. This is because fuzzy logic has been placed to work more sensitive in the range of [0 1], where fuzzy logic will decide a smaller but precise size of perturbed voltage when the PV array is approaching MPP.

The membership functions of the input variables are matched with the membership functions of the output variable forming fuzzy rule base system. The rules are validated through fuzzy viewer by adjusting the index line. This process is to verify the fuzzy computed AV to be same as the desired value.

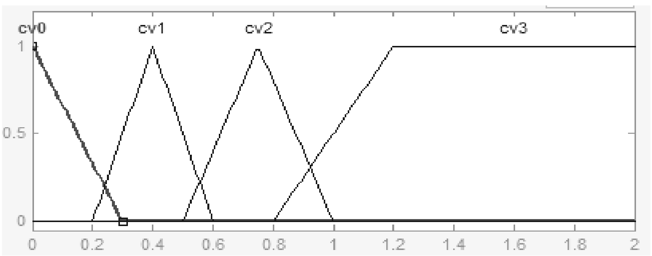

Fig. Membership function of the fuzzy output variable *AV*

## VI SIMULATION RESULTS

In this section several simulation results will be presented. The simulated PV system is a 3 2 PV array, whose parameters are listed in Tables I and II.

The PV array is connected to a boost DC-DC converter which tracks the maximum power point. There are three series connected 12-V batteries in the output side. The parameters of system under study are listed in Table III. Also the schematic of the system is shown in Fig. 6.

During adoption of HC method, the duty cycle of the boost converter is calculated directly based on the last duty cycle as follows:

$$Dk = Dk - 1 + dk \qquad (22)$$

where *D* and *D* are the calculated duty cycles in previous (k-1 th) and present (kth) cycle, respectively.dk is a number which it's value is constant, but it's sign may change in each cycle. If the value of the power measured in the *K*th cycle is larger than the value of power measured in (*K*-1)th cycle, *dk* is calculated as

$$Dk = Dk - 1 \qquad (23)$$

On the other hand, if the power in the *K*th cycle is smaller than the power in (*K*-1)th cycle, *dk* is calculated as

$$Dk = -Dk - 1 \qquad (24)$$

Also, when a reference voltage (Vref) is chosen in global MPPT subroutine, the duty cycle (D∗) is generated as follows [7]:

$$D^* = 1 - Vref/Vout \qquad (25)$$

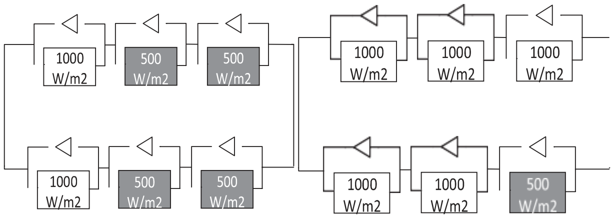

(a) (b)

Fig. 7. PSC patterns in the first simulation, (a) from 0.3 to 0.6 s and (b)

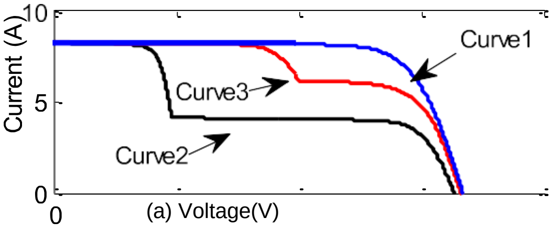

from 0.6 to 0.9 s.

Fig. 8. Corresponding (a) I-V and (b) P-V characteristics under first

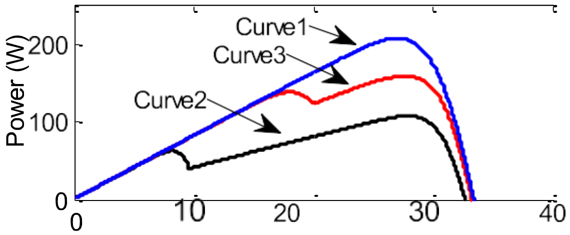

simulation

## VII PERFORMANCE EXPLORATION UNDER FOUR CONSECUTIVE SOLAR IRRADIANCE CONDITION:

In this section, the performance of the algorithm is tested under four consecutive solar irradiance conditions. From 0 to 0.3 s, the solar irradiance level is equal to 1000 W/m$^2$ for all the modules. From 0.3 to 0.6 s and 0.6 to 0.9 s, the solar irradiances are shown in Fig. 7(a) and (b), respectively. Finally, from 0.9 to 1.2 s the solar irradiance is equal to 1000 W/m$^2$ for all the modules again. The I-V and P-V curves of the PV array in these four states are shown in Fig. 8. Array's corresponding voltage, current, power and duty cycle waveforms are shown in Fig. 9(a)–(d), respectively. Moreover, zoomed view of per unit array's voltage, current, power, and duty cycle waveforms in 0.3 to 0.5 s, 0.6 to 0.8 s, and 0.9 to 1.1 s intervals are depicted in Fig. 10(a)–(c), respectively. As illustrated in Fig. 9(c), the algorithm operates properly under normal conditions and the GP is equal to 208 W which is so close to the peak of curve 1 in Fig. 8(b). It is illustrated in Fig. 10(a) that when the solar irradiance level changes at 0.3 s, the proposed method m×easures current in $2 * V_{oc,m}$ , $1 * V_{oc,m}$ ,

and $0.5 * V_{oc,m}$ . Since first and second measured currents are very close and the third differs from these currents, the method recognizes that there are two LPs near $1 \times 0.8 \times V_{oc,m}$ and $3 \times 0.8 \times V_{oc,m}$

. The algorithm performs HC and tracks two LPs with 59.5 and 107 W power which are very close to the peaks of curve 2 in Fig. 8(b), i.e., 63 and 108 W. So the proposed method chooses the biggest LP and continues to work around 107 W.

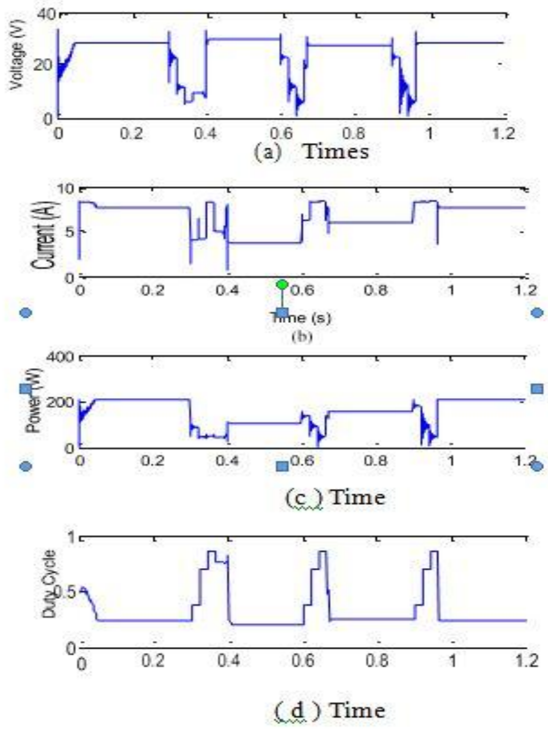

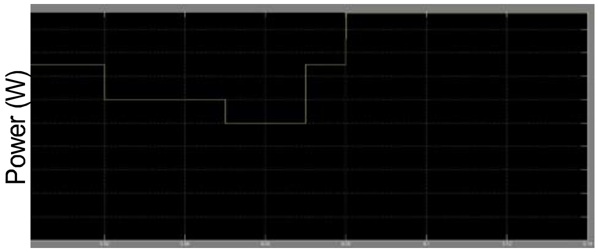

FMPPT

Fig. 9. Corresponding array's (a) voltage, (b) current, (c) power, and (d) duty cycle waveforms in the first simulation

Fig. 10(b) shows that when the solar irradiance changes again at 0.6 s, the proposed method starts to measures current in $2*V_{oc,m}$ , $1*V_{oc,m}$ , and $0.5*V_{oc,m}$ . In this case, second and third measured currents are very close and the first one differs from these currents. Thus, the method recognizes that there are two LPs near 2 0.8 $V_{oc,m}$ and 3 0.8 $V_{oc,m}$ . The algorithm performs HC and tracks two LPs with 139 and 158 W power which are very close to the peaks of curve 3 in Fig. 8(b), i.e., 139 and 159 W. Therefore, the proposed method chooses the biggest LP and continues to work around 159 W.

As it is shown in Fig. 10(c), when the PSC is removed at0.9 s, the proposed method starts to measures the current in $2*V_{oc,m}$ , $1*V_{oc,m}$ , and $0.5*V_{oc,m}$ . In this case, all measured currents are very close. Hence, the method recognizes that there is just one LP near $3 * 0.8 * V_{oc,m}$ . The algorithm operates HC and tracks the LP with 208 W power which is very close to the peak of curve 1 in Fig. 8(b). So the proposed method continues to work around 208 W.

## VIII COMPARISON OF THE NEW METHOD AGAINST OTHER METHODS:

As it was mentioned before, although a large amount of studies is presented in this field, proposing a method which meets accuracy, convergence speed, simplicity, minimum needed parameters, and other important factors is still of a great importance. In this section,

simulations are done to compare the new method against two highly cited methods to show its benefits over those. It should be considered that prior works, such as [17], has shown that some of main hypothesis in [7] are not correct, and it may fail to track the GP in some conditions. However, still [7] is now a classic and highly cited method, and most algorithms are compared to it. For comparing the pro- posed method against [7] and [11], a PSC pattern depicted in Fig. 11(a) is applied to the PV array. The corresponding P-V curve is shown in Fig. 11(b). Also, the corresponding power waveforms of the proposed method, [7] and [11] are illustrated in Fig. 12(a)–(c), respectively.

It is illustrated in Fig. 12(a) that the proposed method tracks the GP with corresponding 97 W power within 0.093 s. The method proposed in [7] tracks the same peak [i.e., the GP in Fig. 11(b) with 99 W power], but in a longer time which is 0.103 s.

Although the method in [11] is faster than two other methods and tracks the peak within 0.077 s, it fails to track the GP correctly. It tracks the middle LP in the P-V curve (87.5 W) instead of the GP. So, it is proved that the proposed method in this paper has good performance in both speed and accuracy factors in comparison to two highly cited methods.

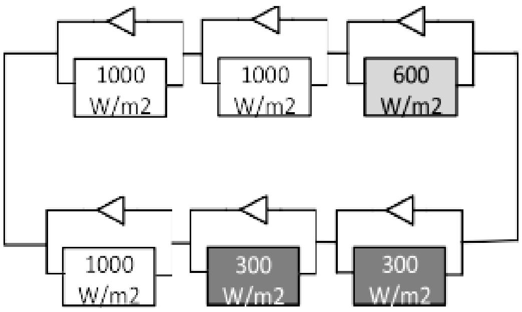

(a)

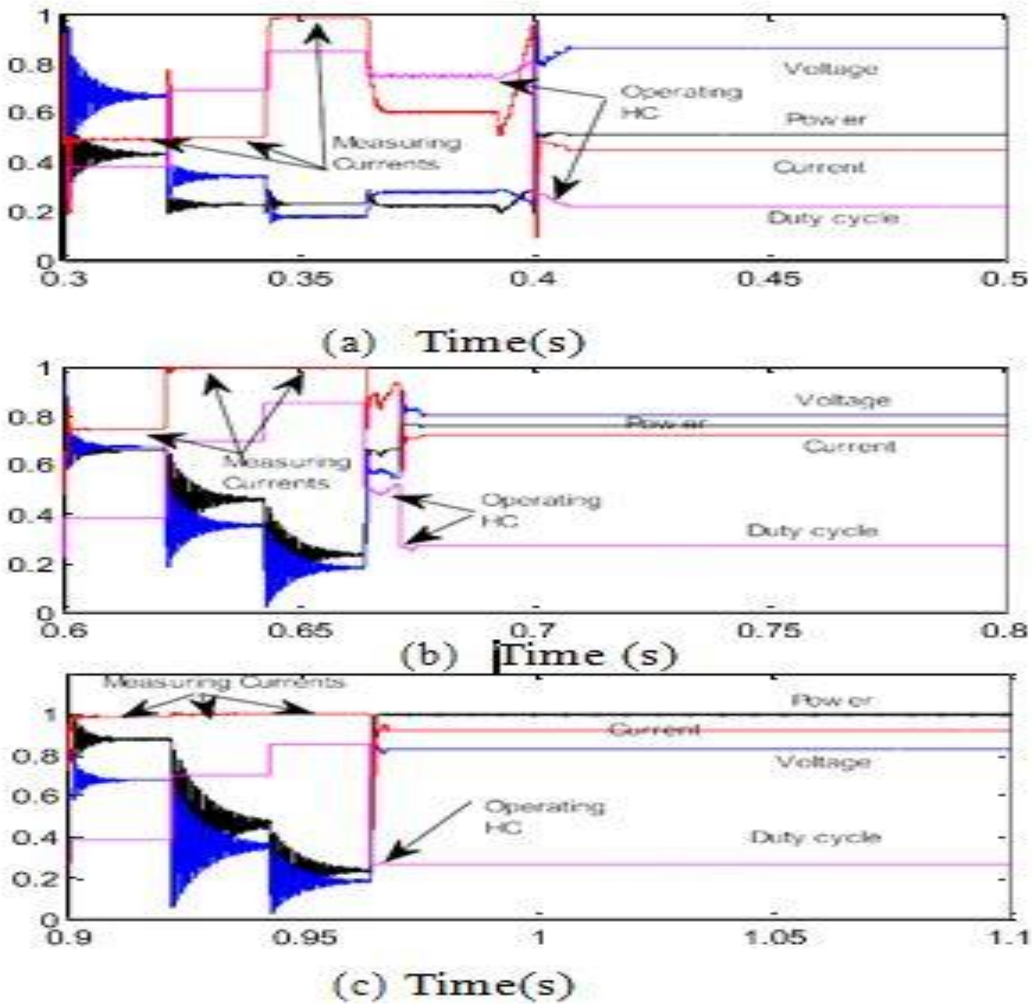

Fig. 10. Zoomed view of per unit array's voltage, current, power, and duty cycle waveforms in the first simulation during (a) 0.3–0.5 s, (b) 0.6–0.8 s, and (c) 0.9–1.1 s intervals. Power should be multiplying to 35 × 6, voltage should be multiplied to 3 × 11.15 and current should be multiplied to 2 × 4.15.

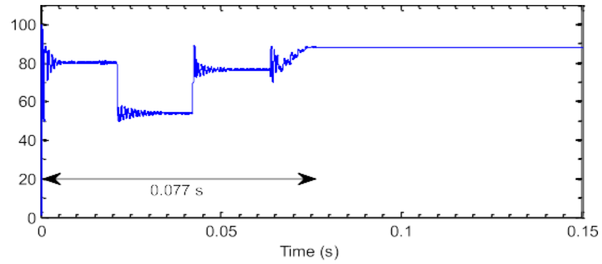

(c)

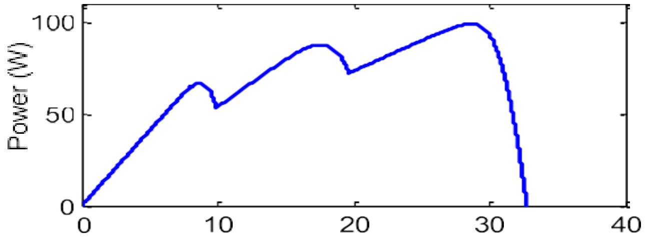

( b ) Voltage

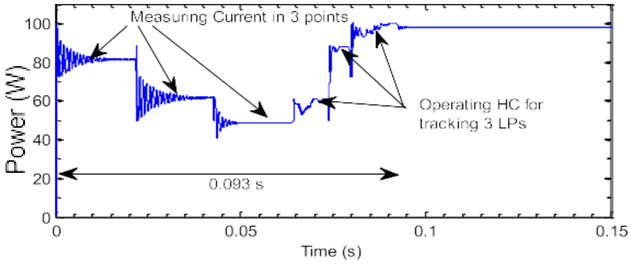

(a)

Fig. 11. Corresponding (a) PSC pattern and (b) P- V characteristics under second simulation.

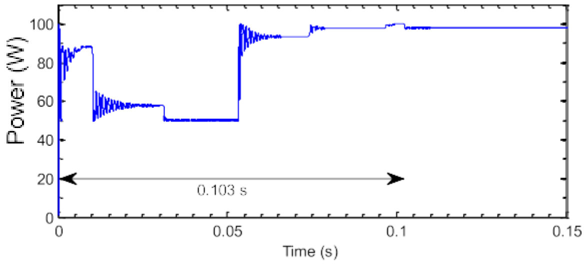

(b)

Fig. 12. Comparison of the performance of (a) the proposed method, (b) the proposed method in [7], and

(c) the proposed method in [11].

## IX CONCLUSION

In this paper, a novel MPPT method was proposed which has a great performance under PSC. Based on the simulation and experimental results, it was shown that the current in each step of the I-V characteristic is almost constant until the beginning point of the next step. In addition, it was proved that starting points of each step in the I-V curve are in near left side neighborhood of the multiples of Voc, m.

The proposed method is in fact, a modified HC method which tracks the GP effectively under different conditions. Thus, the implementation of this method is simple. Once the PSCs appear, the number and length of I-V characteristic's steps are recognized by measuring the current valve in multiples of 0.8*Voc, m. The HC method tracks all LPs. Finally, the GP is detected by comparing the LPs. Simulation and experimental results have validated the advantages of this method in terms of accuracy and speed over two popular existing methods.

## REFERENCES

[1] T. Esram and P. L. Chapman, "Comparison of photovoltaic array maximum power point tracking techniques," IEEE Trans. Energy Convers., vol. 22, no. 2, pp. 439–449, Jun. 2007.

[2] K. Ishaque and Z. Salam, "A review of maximum power point track- ing techniques of PV system for uniform

insolation and partial shading condition," Renew. Sustain. Energy Rev., vol. 19, pp. 475–488, Mar. 2013.

[3] L. Liqun, X. Meng, and C. Liu. "A review of maximum power point tracking methods of PV power system at uniform and partial shading," Renew. Sustain. Energy Rev., vol. 53, pp. 1500– 1507, Jan. 2016.

[4] A. Kouchaki, H. Iman-Eini, and B. Asaei, "A new maximum power point tracking strategy for PV arrays under uniform and non-uniform insolation conditions," Solar Energy, vol. 91, pp. 221–232, May 2013.

[5] R. C. Pilawa-Podgurski and D. J. Perreault, "Submodule integrated distributed maximum power point tracking for solar photovoltaic applications," IEEE Trans. Power Electron., vol. 28, no. 6, pp. 2957–2967, Jun. 2013.

[6] C. Woei-Luen and C. Tsai. "Optimal balancing control for tracking theoretical global MPP of series PV modules subject to partial shading." IEEE Trans. Ind. Electron., vol. 62, no. 8, pp. 4837–4848, Aug. 2015

[7] H. Patel and V. Agarwal, "Maximum power point tracking scheme for PV systems operating under partially shaded conditions," IEEE Trans. Ind. Electron., vol. 55, no. 4, pp. 1689–1698, Apr.

2008.

[8] J. Qi, Y. Zhang, and Y. Chen, "Modeling and maximum power point tracking (MPPT) method for PV array under partial shade conditions," Renew. Energy, vol. 66, pp. 337–345, Jun. 2014.

[9] E. Koutroulis and F. Blaabjerg, "A new technique for tracking the global maximum power point of PV arrays operating under partial-shading conditions," IEEE J. Photovoltaic., vol. 2, no. 2, pp. 184–190, Apr. 2012.

[10] KS. Tey and S. Mekhilef, "Modified incremental conductance algorithm for photovoltaic system under partial shading conditions and load variation," IEEE Trans. Ind. Electron., vol. 61, no. 10, pp. 5384–5392, Oct. 2014.

[11] M. Boztepe, F. Guinjoan, G. Velasco-Quesada,

S. Silvestre, A. Chouder, and E. Karatepe, "Global MPPT scheme for photovoltaic string inverters based on restricted voltage window search algorithm," IEEE Trans. Ind. Electron., vol. 61, no. 7, pp. 3302–3312, Jul. 2014.

[12] K. Chen, S. Tian, Y. Cheng, and L. Bai, "An improved MPPT controller for photovoltaic system under partial shading condition," IEEE Trans. Sustain. Energy, vol. 5, no. 3, pp. 978–985,

Jul. 2014

[13] W. Yunping, Y. Li, and X. Ruan, "High-accuracy and fast-speed MPPT methods for PV string under partially shaded conditions," IEEE Trans. Ind. Electron., vol. 63, no. 1, pp. 235–245, Jan. 2016.

[14] M. A. Ghasemi, H. Mohammadian Forushani, and M. Parniani. "Partial shading detection and smooth maximum power point tracking of PV arrays under PSC," IEEE Trans. Power Electron., vol. 31, no. 9, pp. 6281–6292, Sep. 2016.

[15] P. Lei, Y. Li, and J. E. Seem, "Sequential ESC- Based Global MPPT Control for Photovoltaic Array with Variable Shading," IEEE Trans. Sustain. Energy, vol. 2, no. 3, pp. 348–358, Jul. 2011.

[16] M. G. Villalva and J. R. Gazoli, "Comprehensive approach to modeling and simulation of photovoltaic arrays," IEEE Trans. Power Electron., vol. 24, no. 5, pp. 1198–1208, May 2009.

[17] S. Kazmi, H. Goto, O. Ichinokura, and H. J. Guo. "An improved and very efficient MPPT controller for PV systems subjected to rapidly varying atmospheric conditions and partial shading," in Proc. Australasian Univ. Power Eng. Conf., 2009, pp. 1–6.